Are There Stable Ion-Pairs in Room-Temperature Ionic Liquids? Molecular Dynamics Simulations of 1-n-Butyl-3-methylimidazolium Hexafluorophosphate

7 AUTHORS, INCLUDING:

Frédéric Leroy
Universität Kassel

38 PUBLICATIONS   **706** CITATIONS

SEE PROFILE

Berit Heggen
Max Planck Institute for Empirical Aesthetics

10 PUBLICATIONS   **205** CITATIONS

SEE PROFILE

Stefan Zahn
University of Leipzig

38 PUBLICATIONS   **1,033** CITATIONS

SEE PROFILE

Barbara Kirchner
University of Bonn

201 PUBLICATIONS   **4,516** CITATIONS

SEE PROFILE

Are There Stable Ion-Pairs in Room-Temperature Ionic Liquids? Molecular Dynamics Simulations of 1-*n*-Butyl-3-methylimidazolium Hexafluorophosphate

Wei Zhao,*,† Frédéric Leroy,† Berit Heggen,† Stefan Zahn,‡ Barbara Kirchner,‡ Sundaram Balasubramanian,§ and Florian Müller-Plathe†

Eduard-Zintl-Institut für Anorganische und Physikalische Chemie, Technische Universität Darmstadt, Petersenstrasse 20, D-64287 Darmstadt, Germany, Wilhelm-Ostwald Institute of Physical and Theoretical Chemistry, University of Leipzig, Linnéstrasse 2, D-04103 Leipzig, Germany, and Chemistry and Physics of Materials Unit, Jawaharlal Nehru Centre for Advanced Scientific Research, Jakkur, Bangalore 560 064, India

Received July 28, 2009; E-mail: w.zhao@theo.chemie.tu-darmstadt.de

Abstract: Molecular dynamics simulations with an all-atom model were carried out to study the ionic liquid 1-*n*-butyl-3-methylimidazolium hexafluorophosphate, [bmim][PF$_6$]. Analysis was carried out to characterize a number of structural and dynamic properties. It is found that the hydrogen bonds are weaker than expected, as indicated by their short lifetimes, which is due to the fast rotational motion of anions. Transport properties such as ion diffusion coefficients and ionic conductivity were also measured on the basis of long trajectories, and good agreement was obtained with experimental results. The phenomenon that electrical conductivity of ionic liquids deviates from the Nernst−Einstein relation was well reproduced in our work. On the basis of our analysis, we suggest that this deviation results from the correlated motion of cations and anions over time scales up to nanoseconds. In contrast, we find no evidence for long-lived ion-pairs migrating together.

Introduction

Ionic liquids represent a class of chemicals to which intensive research activity has been devoted in recent years.[1−3] With properties such as near-zero vapor pressure, nonflammability, chemical and thermal stability, and conductivity, ionic liquids have been introduced into a number of industrial applications.[4] There are, however, still obstacles which prevent further utilization. Major ones are their poor transport properties such as high viscosity and low electrical conductivity, which limit their use as reaction media or as electrolytes. The design of more suitable ionic liquids with the desired transport properties will probably benefit from a better understanding of cation−anion interactions at the molecular level.[2,5] The chemical constitution of ionic liquids determines the nature of cation−anion interactions and thus the macroscopically observable properties such as thermodynamic and transport properties. For example, as reported by Canongia Lopes and Pádua,[6] nanostructural organization of ionic liquids results in three-dimensional networks of ionic channels and nonpolar domains, which have been suggested to affect viscosity, diffusion, and ionic conductivity.

Recent work by Hu and Margulis also suggested that the slow dynamics in ionic liquids is related to the existence of locally heterogeneous environments.[7] Moreover, the molecular nature of the ions and their asymmetric shapes cause asymmetric ion−ion distributions in the molecular interactions. Furthermore, the short-range interactions may be highly directional and the electrostatic interactions may be weakened by charge screening by the first neighbors.[2,8] Thus, van der Waals interactions between groups having less dominant electrostatic interaction should also be taken into account. Therefore, a deeper understanding of the effects of structure on other properties of ionic liquids is of great significance.

Among the features of cation−anion interactions, the alleged formation of ion-pairs has attracted much attention recently, because the intense attractive interaction between ions is expected to yield long-lived association of ions. There are, however, questions remaining about the nature and the precise origin of this possible association. It has been suggested by some authors that cations and anions are bonded to ion-pairs through hydrogen bonds for some ionic liquids such as [emim][Tf$_2$N][9] and [bmim][Cl],[10,11] in which the existence of hydrogen bonds of high binding energy between cation and anion has been shown in the gas phase. For example, the 1-*n*-butyl-3-methylimidazolium hexafluorophosphate ([bmim][PF$_6$]) ionic liquid

---

† Technische Universität Darmstadt.
‡ University of Leipzig.
§ Jawaharlal Nehru Centre for Advanced Scientific Research.
(1) Wasserscheid, P.; Keim, W. *Angew. Chem., Int. Ed.* **2000**, *39*, 3772.
(2) Weingärtner, H. *Angew. Chem., Int. Ed.* **2008**, *47*, 654.
(3) Welton, T. *Chem. Rev.* **1999**, *99*, 2071.
(4) Rogers, R. D.; Seddon, K. R. *Science* **2003**, *302*, 792.
(5) Lynden-Bell, R. M.; del Popolo, M. G.; Youngs, T. G. A.; Kohanoff, J.; Hanke, C. G. *Acc. Chem. Res.* **2007**, *40*, 1138.
(6) Canongia Lopes, J. N.; Pádua, A. A. H. *J. Phys. Chem. B* **2006**, *110*, 3330.

(7) Hu, Z.; Margulis, C. J. *Acc. Chem. Res.* **2007**, *40*, 1097.
(8) Kobrak, M. N. *J. Phys. Chem. B* **2007**, *111*, 4755.
(9) Ködderman, T.; Wertz, C.; Heintz, A.; Ludwig, R. *ChemPhysChem* **2006**, *7*, 1944.
(10) Hunt, P. A.; Gould, I. R.; Kirchner, B. *Aust. J. Chem.* **2007**, *60*, 9.
(11) Hunt, P. A.; Kirchner, B.; Welton, T. *Chem.−Eur. J.* **2006**, *12*, 6762.

investigated here could show hydrogen bonds between the imidazolium ring and the fluorine atoms of PF_6^-. However, the relative importance of the hydrogen-bonding interaction is still subject to discussion. While some authors attribute a crucial role to it,[12] others consider its relevance minor compared with the role of the pure electrostatic interaction.[2,13,14] It was found by Armstrong et al.[15] using mass-spectrometric methods that the vapor phase of ionic liquids contains ion-pairs. Ion-pairs were also discovered to exist in dilute solutions of ionic liquids both in experiments[16,17] and in molecular dynamics simulations.[18]

However, it is still under debate whether ion-pairs exist in ionic liquids in the bulk liquid phase or, in fact, if the concept of ion-pairs makes sense in neat ionic liquids. Some authors argue that cations and anions form ion-pairs even in the liquid phase due to their strong opposite charges.[19-21] This point of view is supported by the fact that the conductivity of ionic liquids generally deviates from the Nernst−Einstein approximation,[20,22,23] which can be easily explained as reduction of the effective number of ions available for conduction through formation of ion-pairs having a zero net charge. On the other hand, there is no solid evidence for the existence of long-lived ion-pairs in the liquid phase. For instance, dielectric spectroscopy has shown that, for the studied ionic liquids, ion-pairs with a lifetime ranging from picoseconds to nanoseconds do not exist.[17,24-26] In a simulation study, del Popolo and Voth[27] suggested that the reduction in conductivity might result from the short correlation in the motion of neighboring cations and anions at a subpicosecond time scale. A similar view on short-lived correlation among ions was also proposed by Hansen and McDonald[28] in 1975 in a molecular dynamics study on simple molten salt to explain deviation from the Nernst−Einstein relation for system such as liquid NaCl, CsCl, and $LiNO_3$. Other theoretical concepts, for example similar to the electrostatic drag in dilute solutions of strong electrolytes, which is well described by the Debye−Hückel−Onsager theory,[29] are possible alternative explanations for the deviation from Nernst−Einstein

behavior. To settle this debate, further investigation of cation−anion interactions at the molecular level is needed. The theoretical tools to describe ion-pairing that have been developed in the context of dilute solutions[18,30] may not be adaptable because neighborhoods of ions in neat ionic liquids present significant fluctuations of the local charge density which is not present in dilute solutions. Therefore, other tools have to be developed and used.

Molecular dynamics has already proven itself to be a powerful tool for the investigation of a number of ionic liquid systems and has yielded knowledge that is not available experimentally. To date, extensive classical molecular dynamics (MD) simulation studies have been performed on a number of ionic liquids[5-7,9,18,27,30-55] since the first MD simulation performed by Hanke et al. in 2001.[43]

In the present work, the ionic liquid [bmim][PF_6] (see Figure 1) was studied using MD simulations. In our work, through detailed analysis of a series of structural and dynamic properties including structure, formation of hydrogen bonds, and transport properties as well as cation−anion interactions, we aim to obtain further knowledge about the ion-pairing which is difficult to obtain experimentally.

Model Description and Computational Methods

The force field of the ionic liquid [bmim][PF_6] was taken from the model of Bhargava and Balasubramanian.[40] This is a nonpo-

(12) Dupont, J. *J. Braz. Chem. Soc.* **2004**, *15*, 341.
(13) Tsuzuki, S.; Tokuda, H.; Mikami, M. *Phys. Chem. Chem. Phys.* **2007**, *9*, 4780.
(14) Schröder, C.; Rudas, T.; Steinhauser, O. *J. Chem. Phys.* **2006**, *125*, 244506.
(15) Armstrong, J. P.; Hurst, C.; Jones, R. G.; Licence, P.; Lovelock, K. R. J.; Satterley, C. J.; Villar-Garcia, I. J. *Phys. Chem. Chem. Phys.* **2007**, *9*, 982.
(16) Tubbs, J. D.; Hoffmann, M. M. *J. Solution Chem.* **2004**, *33*, 381.
(17) Schrödel, S.; Annat, G.; MacFarlane, D. R.; Forsyth, M.; Buchner, M.; Hefter, G. *Chem. Commun.* **2006**, 1748.
(18) del Popolo, M. G.; Mullan, C. L.; Holbrey, J. D.; Hardacre, C.; Ballone, P. *J. Am. Chem. Soc.* **2008**, *130*, 7032.
(19) Katoh, R.; Hara, M.; Tsuzuki, S. *J. Phys. Chem. B* **2008**, *112*, 15426.
(20) Tokuda, H.; Ishii, K.; Susan, A. B. H.; Tsuzuki, S.; Hayamizu, K.; Watanabe, M. *J. Phys. Chem. B* **2006**, *110*, 2833.
(21) Every, H. A.; Bishop, A. G.; MacFarlane, D. R.; Oraedd, G.; Forsyth, M. *Phys. Chem. Chem. Phys.* **2004**, *6*, 1758.
(22) Tokuda, H.; Hayamizu, K.; Ishii, K.; Susan, A. B. H.; Watanabe, M. *J. Phys. Chem. B* **2004**, *108*, 16593.
(23) Tokuda, H.; Ishii, K.; Susan, A. B. H.; Tsuzuki, S.; Hayamizu, K.; Watanabe, M. *J. Phys. Chem. B* **2005**, *109*, 6103.
(24) Schröder, C.; Wakai, D.; Weingärtner, H.; Steinhauser, O. *J. Chem. Phys.* **2007**, *126*, 084511.
(25) Daguenet, C.; Dyson, P. J.; Krossing, I.; Slattery, J. M.; Oleinikova, A.; Wakai, D.; Weingärtner, H. *J. Phys. Chem. B* **2006**, *110*, 12682.
(26) Weingärtner, H.; Daguenet, C.; Dyson, P. J.; Krossing, I.; Slattery, J. M.; Schubert, T. *J. Phys. Chem. B* **2007**, *111*, 4775.
(27) del Popolo, M. G.; Voth, G. A. *J. Phys. Chem. B* **2004**, *108*, 1744.
(28) Hansen, J. P.; McDonald, I. R. *Phys. Rev. A* **1975**, *11*, 2111.
(29) Atkins, P.; de Paula, J. *Physical Chemistry*, 8th ed.; Oxford University Press: Oxford, UK, 2006.

(30) Köddermann, T.; Ludwig, R.; Paschek, D. *ChemPhysChem* **2008**, *9*, 1851.
(31) de Azevedo, R. G.; Esperanca, J. M. S. S.; Szydlowski, J.; Visak, Z. P.; Pires, P. F.; R., G. H. J.; Rebelo, L. P. N. *J. Chem. Thermodyn.* **2005**, *37*, 888.
(32) Borodin, O.; Smith, G. D. *J. Phys. Chem. B* **2006**, *110*, 11481.
(33) Canongia Lopes, J. N.; Deschamps, J.; Pádua, A. A. H. *J. Phys. Chem. B* **2004**, *108*, 2038.
(34) Canongia Lopes, J. N.; Deschamps, J.; Pádua, A. A. H. *J. Phys. Chem. B* **2004**, *108*, 11250.
(35) Canongia Lopes, J. N.; Gomes, M. F. C.; Pádua, A. A. H. *J. Phys. Chem. B* **2006**, *110*, 16816.
(36) Canongia Lopes, J. N.; Pádua, A. A. H. *J. Phys. Chem. B* **2004**, *108*, 16893.
(37) Canongia Lopes, J. N.; Pádua, A. A. H. *J. Phys. Chem. B* **2006**, *110*, 19586.
(38) del Popolo, M. G.; Kohanoff, J.; Lynden-Bell, R. M.; Pinilla, C. *Acc. Chem. Res.* **2007**, *40*, 1156.
(39) Bhargava, B. L.; Balasubramanian, S. *J. Am. Chem. Soc.* **2006**, *128*, 10073.
(40) Bhargava, B. L.; Balasubramanian, S. *J. Chem. Phys.* **2007**, *127*, 114510.
(41) Hunt, P. A. *J. Phys. Chem. B* **2007**, *111*, 4844.
(42) Hanke, C. G.; Lynden-Bell, R. M. *J. Phys. Chem. B* **2003**, *107*, 10873.
(43) Hanke, C. G.; Price, S. L.; Lynden-Bell, R. M. *Mol. Phys.* **2001**, *99*, 801.
(44) Sloutskin, E.; Lynden-Bell, R. M.; Balasubramanian, S.; Deutsch, M. *J. Chem. Phys.* **2006**, *125*, 174715.
(45) Lynden-Bell, R. M.; del Popolo, M. G. *Phys. Chem. Chem. Phys.* **2006**, *8*, 949.
(46) Lynden-Bell, R. M.; Kohanoff, J.; del Popolo, M. G. *Faraday Discuss.* **2005**, *129*, 57.
(47) Lynden-Bell, R. M.; Youngs, T. G. A. *Mol. Sim.* **2006**, *32*, 1025.
(48) Zhao, W.; Leroy, F.; Balasubramanian, S.; Müller-Plathe, F. *J. Phys. Chem. B* **2008**, *112*, 8129.
(49) Zhao, W.; Eslami, H.; Cavalcanti, W. L.; Müller-Plathe, F. *Z. Phys. Chem* **2007**, *221*, 1647.
(50) Cadena, C.; Maginn, E. J. *J. Phys. Chem. B* **2006**, *110*, 18026.
(51) Cadena, C.; Anthony, J. L.; Shah, J. K.; Morrow, T. I.; Brennecke, J. F.; Maginn, E. J. *J. Am. Chem. Soc.* **2003**, *126*, 5300.
(52) Cadena, C.; Zhao, Q.; Snurr, R. Q.; Maginn, E. J. *J. Phys. Chem. B* **2006**, *110*, 2821.
(53) de Andrade, J.; Boes, E. S.; Hubbert, S. *J. Phys. Chem. B* **2002**, *106*, 3546.
(54) Kelkar, M. S.; Maginn, E. J. *J. Phys. Chem. B* **2007**, *111*, 4867.
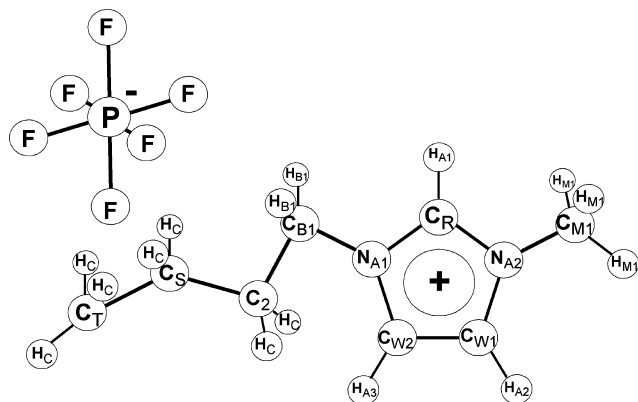(55) Bhargava, B. L.; Balasubramanian, S.; Klein, M. L. *Chem. Commun.* **2008**, *29*, 3339.

Figure 1. Chemical structures of 1-*n*-butyl-3-methylimidazolium ([bmim]) (bottom) and hexafluorophosphate ([PF₆]).

Figure 2. Electrostatic potential at the isodensity surface with 0.05 *e*/bohr³ for [bmim] (left) and [PF₆] (right).

Figure 3. Spatial distribution functions (SDFs) of fluorine atoms of the anions around a cation: (a) with isosurface value of 0.025 Å⁻³ and (b) with isosurface value of 0.0377 Å⁻³.

larizable model in which the total charge on the [bmim] cation and [PF₆] anion have been chosen to be 0.8 e and −0.8 e, respectively. A cutoff of 1.2 nm was applied for the nonbonded interactions. Mixed Lennard-Jones parameters were derived from self-parameters using the Lorenz–Berthelot mixing rules.[56] Within one molecule, 1-2 and 1-3 nonbonded interactions were excluded, and 1-4 nonbonded interaction strengths were divided by a factor of 2, as is usual in all-atom OPLS-type force fields.[57] The reaction-field method with a dielectric constant $\epsilon_{RF} = 11.4$ was employed to compute electrostatic interactions.[58] The SHAKE algorithm was used to constrain all bonds.

The MD simulations were performed at 300, 320, 340, 360, and 380 K. The periodic simulation box containing 256 pairs of [bmim] cations and [PF₆] anions (8192 atoms) was taken from our previous work. The system was simulated for 50 ns at 300 K and for 40 ns at higher temperatures with a time step of 2 fs. The neighbor list was updated every 15 time steps. The first 10 ns of each trajectory was used for equilibration, and the rest of the time was used for data analysis. In all simulations, the temperature was kept constant using the Berendsen thermostat and barostat[59] with coupling times of 0.2 and 2.0 ps, respectively. All simulations were performed using our molecular simulation package YASP.[60,61]

In calculation of electrostatic potentials, geometry optimizations were carried out using the BLYP-D[62−64] density functional using the TZVPP[65] basis set with the resolution of identity (RI). The convergence criterion of the iteration cycle was increased to 10^{-8} hartree for all calculations.

Results

A. Structure. In an ionic liquid system, cation−anion interactions are largely determined by the balance among electrostatic properties, van der Waals interactions, and the geometrical properties of both cations and anions. Figure 2 shows the electrostatic potentials for both a [bmim] cation and a [PF₆] anion. A high electrostatic potential (positive, red color) is evident for the cation due to its overall positive charge in comparison with low (negative) electrostatic potential found for
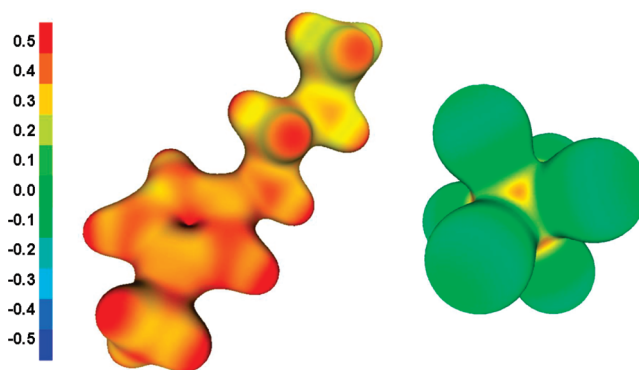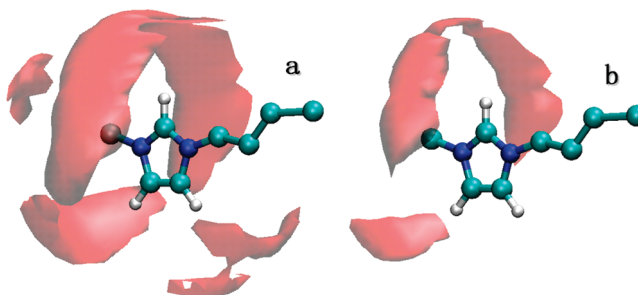
fluorine atoms of the anion as a consequence of their negative charge. Due to the high potential, the methyl groups as well as the hydrogen atoms on the imidazolium ring are favorable for interactions with anions. The imidazolium hydrogens (i.e., H_{A1}, H_{A2}, and H_{A3}, see Figure 1) should additionally be able to form hydrogen bonds, as also proposed by previous quantum calculations.[9,10] In particular, a positive electrostatic potential was found around the carbons on the imidazolium ring, especially at C_R. This makes them different from traditional hydrogen donors, such as water oxygen, which typically bear a negative potential. The impact of the electrostatic properties of the cations and anions will be addressed in the following sections.

The preference of these sites for interaction with the anion is confirmed by the spatial distribution function (SDF) of anions around the cation (Figure 3), which has been reported for an isosurface value of 0.0375 Å⁻³ for the current model in a previous study.[40] Here we recalculated it at different isosurface values in order to support our discussion (see Figure S1 in Supporting Information). According to the probability density to find fluorine atoms of the anions around a cation, three main types of cation−anion contact can be classified. The most prominent region to find an anion is above and below the imidazolium ring. The region with secondary density is around H_{A1} and H_{A2}. The contact region around H_{A1} connects the two regions above and below the imidazole ring into a single semicircular region. The third type of contact region is found around the methyl group and H_{A3}.

Figure 4 shows the radial distribution functions (RDFs) of anions (P atom) with respect to different sites of the cations. The RDF to the ring center of the cation is characterized by a strong peak around 0.52 nm with two shoulders, one at 0.45 nm and one at 0.65 nm. A similar feature in RDFs has been

(56) Allen, M. P.; Tildesley, D. J. *Computer Simulation of Liquids*; Oxford University Press: Oxford, UK, 1989.
(57) Jogensen, W. L.; Maxwell, D. S.; Tirado-Rives, J. *J. Am. Chem. Soc.* **1996**, *118*, 11225.
(58) Weingärtner, H. *Z. Phys. Chem* **2006**, *220*, 1395.
(59) Berendsen, H. J. C.; Postma, J. P. M.; van Gunsteren, W. F.; Dinola, A.; Haak, J. R. *J. Chem. Phys.* **1984**, *81*, 3684.
(60) Müller-Plathe, F. *Comput. Phys. Commun.* **1993**, *78*, 77.
(61) Tarmyshov, K.; Müller-Plathe, F. *J. Chem. Inf. Modell.* **2005**, *45*, 1943.
(62) Becke, A. D. *Phys. Rev. A* **1988**, *38*, 3098.
(63) Lee, C.; Yang, W.; Parr, R. G. *Phys. Rev. B* **1988**, *37*, 785.
(64) Grimme, S. *J. Comput. Chem.* **2006**, *27*, 1787.
(65) Weigend, F.; Ahlrichs, R. *Phys. Chem. Chem. Phys.* **2005**, *7*, 3297.
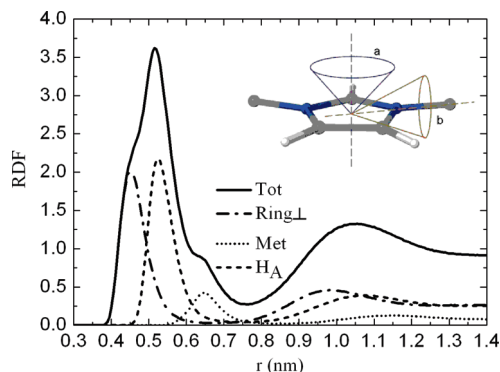
Figure 4. Radial distribution functions (RDFs) between the geometrical center of the anions and the geometrical center of cations' imidazolium rings (denoted as "Tot") and its angle-resolved components. "Ring$_\perp$" refers to the component of the RDF falling into a cone of opening angle 35° around the imidazolium ring plane normal, labeled "a" in the inset. "Met" denotes a cone of an opening angle 35° in the direction of the methyl group, labeled "b" in the inset. "H$_A$" collectively describes similar cones in the direction of the three imidazolium hydrogen atoms H$_{A1}$, H$_{A2}$, and H$_{A3}$.
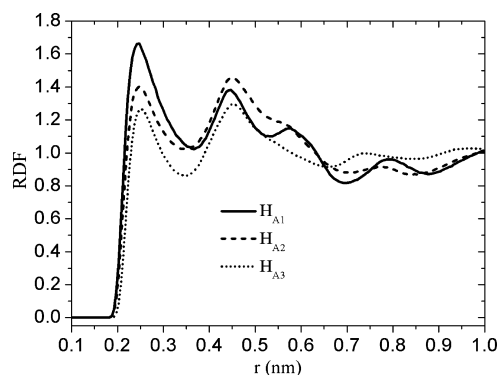

Figure 5. Radial distribution functions (RDFs) between fluorine atoms of [PF$_6$] anion and the individual imidazolium hydrogens of [bmim] cations.

observed in neutron diffraction measurements of [mmim][PF$_6$].[66] For detailed information, this spherically averaged RDF is broken down into several angle-dependent RDFs: The shoulder at 0.45 nm is the closest approach and is due to the anion being located above or below the imidazole ring. The main peak at 0.52 nm is caused by the anion interacting with the imidazolium hydrogen atoms. The shoulder at 0.65 nm belongs to an interaction with the methyl group. These distributions are in line with the spatial distribution functions of anions around the cation (Figure 3). A previous X-ray diffraction experiment on [bmim][PF$_6$] crystals suggested[67] an average separation of positive and negative charge of 0.477 nm, which falls between the RDF peaks at 0.45 and 0.52 nm. As shown in Figure 5, the RDFs between anion fluorine atoms and the ring hydrogens exhibit peaks around 0.244 nm, which suggest the existence of hydrogen bonds. Therefore, an analysis of the strength and population of hydrogen bonds was carried out.

B. Characterization of Hydrogen Bonds. Hydrogen bonds have been suggested to be one of the molecular features which determine the properties of ionic liquids.[1,9] Some authors claimed that strong hydrogen-bonding can be the reason for the
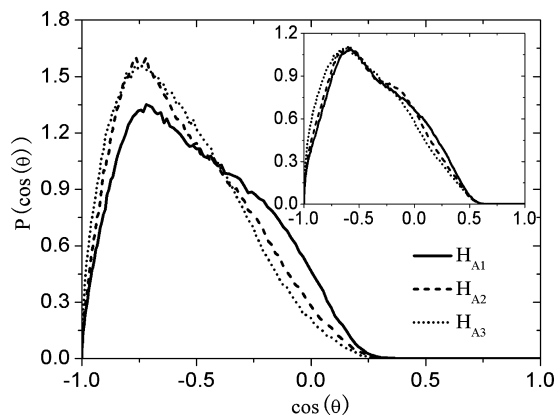
(66) Hardacre, C.; Holbrey, D.; Nieuwenhuyzen, M.; Youngs, T. G. A. *Acc. Chem. Res.* **2007**, *40*, 1146.
(67) Kolle, P.; Dronskowski, R. *Eur. J. Inorg. Chem.* **2004**, 2313.

Figure 6. Distribution of the angles between the vectors connecting hydrogen and H-donor (e.g., H$_{A1}$–C$_R$) and hydrogen and anion center, represented by the phosphorus atom. The inset shows the distribution of C–H···F angles. The curves are labeled by the hydrogen involved. The area under each curve is normalized to one.

high viscosity.[1] In the present example of an ionic liquid, the imidazolium ring of the [bmim] cations bears three hydrogen atoms, which are potential hydrogen donors, as indicated by the electrostatic potential maps shown in the previous section. In this study, the hydrogen bonds are formed by the acidic ring protons (e.g., C$_R$, C$_{W1}$, C$_{W2}$) of the [bmim] cations as H-donors and the fluorine atoms of the [PF$_6$] anions as H-acceptors. We first analyze the linearity of the hydrogen bonds formed between cations and anions. Figure 6 shows the distribution of the angles formed by the respective CH bonds (C$_R$, C$_{W1}$, and C$_{W2}$) and the vectors from the corresponding hydrogen (H$_{A1}$, H$_{A2}$, and H$_{A3}$) to the anion center (P atom), i.e., the angle C–H···P, for all anions within 0.4 nm of the hydrogens. As indicated by Figure 6, the anions interacting with H$_{A1}$ are less localized than those interacting with H$_{A2}$ and H$_{A3}$. This has also been revealed in previous work by Bhargava and Balasubramanian, who found a band-like anion-rich region around H$_{A1}$.[40] The inset of Figure 6 shows the distribution of the C–H···F angle for fluorine atoms to be within 0.35 nm of the hydrogen (first minimum of the RDF, see Figure 5). This angle distribution shows again a domination of large angles which approach linearity. There is, however, also a population of angles around 90° which is larger than in the case of the CH···P angles. This would be compatible with a situation where the anion center is predominantly located collinearly with the CH bond, but with some F atoms rotated away from this axis. This could be the case if the anion were constantly rotating or if one hydrogen were to form bifurcated hydrogen bonds to two fluorines.

We have therefore analyzed the hydrogen bonds formed by the ring hydrogens. The presence of a hydrogen bond is defined if two criteria are satisfied: (1) the C–H···F angle is larger than or equal to 120° and (2) the distance between the hydrogen atom and fluorine is less than or equal to a threshold value of 0.35 nm (minimum of the H–F radial distribution function after the first neighbor shells, Figure 4). On average, H$_{A1}$, H$_{A2}$, and H$_{A3}$ form 1.61, 1.47, and 1.35 bonds, respectively, which amount to a total of 4.44 hydrogen bonds per cation at 300 K. The fact that every ring hydrogen has, on average, hydrogen bonds to more than one fluorine corroborates the above view of bifurcated hydrogen bonds from one hydrogen to two fluorines of the same anion. The coordination numbers of H$_{A1}$, H$_{A2}$, and H$_{A3}$ (with all fluorines) are found to be 3.4, 2.9, and 2.6, respectively. Therefore, around half of the fluorines that are located within

the first coordination shell of the ring hydrogens are not considered to form hydrogen bonds with these ring hydrogens, according to our definition of a hydrogen bond. They are in the vicinity but deviate too much from a linear conformation. Earlier quantum calculations for an isolated ion-pair in the gas phase found hydrogen bonds exclusively for H_{A1}.[9] In the bulk, however, our calculations indicate that all three imidazolium hydrogen atoms contribute to hydrogen-bonding in almost equal proportion.

We characterized the dynamical properties of the hydrogen bonds in terms of two time correlation functions (TCFs),[68−72] the continuous time correlation function, $S(t)$, and the intermittent time correlation function, $C(t)$, defined as

$$S(t) = \frac{\langle \delta h(0) \delta H(t) \rangle}{\langle \delta h(0) \delta H(0) \rangle} = \frac{\langle h(0)H(t) \rangle - \langle h \rangle \langle H \rangle}{\langle h \rangle - \langle h \rangle \langle H \rangle} \approx \frac{\langle h(0)H(t) \rangle}{\langle h \rangle} \tag{1}$$

$$C(t) = \frac{\langle \delta h(0) \delta h(t) \rangle}{\langle \delta h^2 \rangle} = \frac{\langle h(0)h(t) \rangle - \langle h \rangle^2}{\langle h \rangle - \langle h \rangle^2} \approx \frac{\langle h(0)h(t) \rangle}{\langle h \rangle} \tag{2}$$

where the population variable $h(t)$ is unity when a particular hydrogen−fluorine (H−F) pair is hydrogen-bonded at time t according to the definition above, and zero otherwise. On the other hand, $H(t) = 1$ if the tagged H−F remains continuously hydrogen-bonded during the time duration t, and zero otherwise. The angle brackets denote an average over all H-donor and H-acceptor pairs and all starting times. The average number of hydrogen bonds is denoted as $\langle h \rangle$. By definition, $C(t)$ describes the probability that a particular tagged hydrogen bond is intact at time t, given that it was intact at time zero (allowing for re-formation after rupture), while $S(t)$ describes the lifetime of a tagged hydrogen bond to first rupture. The relaxation time of $C(t)$ is usually called the structural relaxation time (τ_R) of hydrogen bonds, and the relaxation time of $S(t)$ describes the average lifetime of hydrogen bonds (τ_{HB}). To calculate $C(t)$, trajectories of 60 ps at all temperature were employed with a sampling step of 40 fs. Since $S(t)$ is very sensitive to the short-time motion of atoms, trajectories of 10 ps were sampled every 4 fs at 300−340 K and every 2 fs at 360 and 380 K, which provides high time resolution. Figure 7 shows $C(t)$ and $S(t)$ measured at 300 K for H_{A1}. It is obvious that $S(t)$ decays much faster than $C(t)$. The inset of Figure 7 shows $C(t)$ for H_{A1} at different temperatures. On one hand, one can see that $C(t)$ decays faster at higher temperature. On the other hand, the curves of $C(t)$ exhibit periodic oscillations, which are due to the re-formation of broken hydrogen bonds; the periodicity of around 30 fs and its temperature independence indicate that the reason is vibrations of the H atoms. In our analysis, it was found that $S(t)$ and $C(t)$ cannot be described by a single-exponential function or stretched exponential function.[73] In order to determine τ_R and τ_{HB}, the $S(t)$ and $C(t)$ curves were fitted by three weighted exponentials (with a total weight of one).

In our analysis, Arrhenius behavior was found for both the structural relaxation times and lifetimes of hydrogen bonds (i.e.,
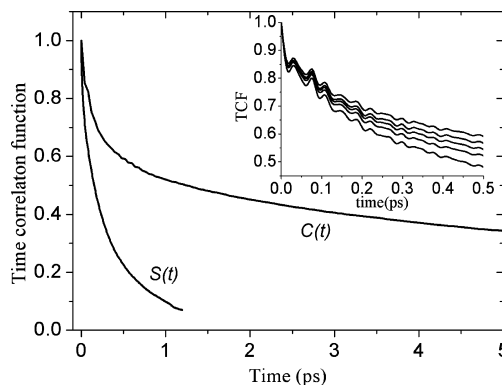

Figure 7. Time correlation functions $S(t)$ and $C(t)$ of the hydrogen bonds formed between H_{A1} and anion fluorine atoms at 300 K. Inset: The same $C(t)$ correlation function at different temperatures (from top to bottom: 300, 320, 340, 360, and 380 K, respectively).

$\tau \propto e^{E_A/k_B T}$, see Figure S1 in Supporting Information). The activation energies associated with the hydrogen bond lifetimes were found to be 4.5 ± 0.4, 4.6 ± 0.2, and 4.8 ± 0.2 kJ mol^{-1} for H_{A1}, H_{A2}, and H_{A3}, respectively (see Table 2, below). The activation energy associated with the hydrogen bond lifetime is interpreted as the energy required to break a hydrogen bond via librational motion. The activation energies associated with structural relaxation times of hydrogen bonds were found to be 9.8 ± 1.2, 10.8 ± 1.1, and 16.1 ± 1.2 kJ mol^{-1} for H_{A1}, H_{A2}, and H_{A3}, respectively. As will be shown below, the magnitude of the activation energy related to the hydrogen bond relaxation time is close to the activation energy for anion reorientation. This is consistent with the concept that the rotation of the anion leads to rapid breaking and forming/re-forming of hydrogen bonds.

The Arrhenius behavior of τ_{HB} of the present ionic liquid system is commonly found also in other hydrogen-bonding fluids such as liquid water in different environments.[74−79] However, it should be pointed out that the charge distribution of cations and anions in ionic liquids is usually more complicated than in small molecules like water or methanol. In ionic liquids, the hydrogen bonds result from the combined interactions of hydrogen-donor and -acceptor groups with the participation of other charged functional groups on the cation and anion as Coulombic interactions are long-ranged. The short lifetimes of the hydrogen bonds seem to indicate that hydrogen bonds will not be the decisive factor in the formation of neutral ion-pairs in ionic liquids, which was also suggested in quantum calculations carried out by Tsuzuki and co-workers on another ionic liquid, [dmim][BF₄].[13]

C. Reorientation Dynamics. The reorientation dynamics of cations and anions is another characteristic of the local dynamic behavior. To this end, the cation backbone is represented by a unit vector **u** pointing from C_{M1} to C_{B1} (Figure 1), and the anion structure is represented by a unit vector pointing from the phosphorus atom to one of the fluorine atoms. From the unit vectors, corresponding time correlation functions $c_1(t) = \langle \mathbf{u}(t) \cdot \mathbf{u}(0) \rangle$ are calculated (see Figure 8). The reorientational

(68) Chandra, A. *Phys. Rev. Lett.* **2000**, *85*, 768.
(69) Karimi-Varzaneh, H. A.; Carbone, P.; Müller-Plathe, F. *Macromolecules* **2008**, *41*, 7211.
(70) Luzar, A.; Chandler, D. *Phys. Rev. Lett.* **1996**, *76*, 928.
(71) Rapaport, D. C. *Mol. Phys.* **1983**, *50*, 1151.
(72) Müller-Plathe, F. *J. Chem. Phys.* **1998**, *108*, 8252.
(73) Chanda, J.; Chakraborty, S.; Bandyopadhyay, S. *J. Phys. Chem. B* **2006**, *110*, 3791.

(74) Starr, F. W.; Nielsen, J. K.; Stanley, H. E. *Phys. Rev. Lett.* **1999**, *82*, 2294.
(75) Chen, S.-H.; Teixeira, J. *Adv. Chem. Phys.* **1985**, *64*, 1.
(76) Conde, O.; Teixeira, J. *Mol. Phys.* **1984**, *53*, 951.
(77) Laenen, R.; Simeonidis, K.; Laubereau, A. *J. Phys. Chem. B* **2002**, *106*, 408.
(78) Luzar, A. *Chem. Phys.* **2000**, *258*, 267.
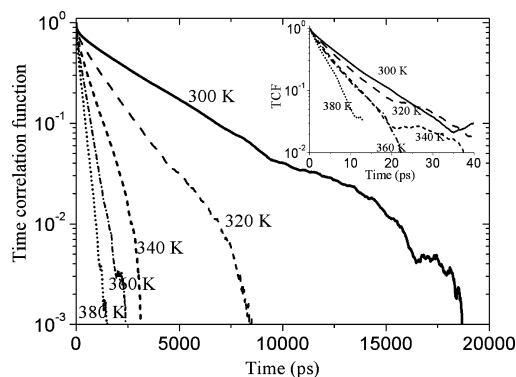(79) Stillinger, F. H. *Science* **1980**, *209*, 451.

Figure 8. Time correlation function for the reorientation of the cations (characterized by unit vector **u** pointing from C_{M1} to C_{B1}) and anions (represented by a unit vector pointing from the phosphorus atom to one of the fluorine atoms) (inset). For the anion reorientation, trajectories of 100 ps sampled every 0.1 ps were used for all systems.

Table 1. Kohlrausch−Willliams−Watts (see Eq 3) Fit Parameters and Time Integrals for the Reorientation Correlation Functions $c_1(t)$ at Different Temperatures

	$C_{M1}-C_{B1}$			P−F		
temp (K)	τ (ps)	α (ps)	β	τ (ps)	α (ps)	β
300	2886	2186	0.67	8.07	7.41	0.85
320	1183	899	0.67	6.65	6.10	0.85
340	523	402	0.68	5.07	4.76	0.88
360	289	229	0.70	4.42	4.16	0.88
380	179	145	0.72	3.47	3.32	0.91

relaxation time τ is given by the time integral $\tau = \int_0^\infty c_1(t)\,\mathrm{d}t$. The integration is performed numerically by first fitting $c_1(t)$ by the Kohlrausch−Williams−Watts (KWW) function:[24]

$$c_1(t) \approx \exp\!\left(\!\left(-\frac{t}{\alpha}\right)^{\beta}\right) \tag{3}$$

where α and β are the fitting parameters. The KWW function has an analytical integral. The fitting parameters are shown in Table 1.

The reorientational relaxation time τ of the cations is much longer than that of the anions at all temperatures. For example, at 300 K τ of the cations was found to be 2886 ps, while that of the anions was 7.4 ps. This suggests much slower rotation of the cations, which is easily explained by their size and asymmetry. A similar faster rotational dynamics of anions was also reported by Steinhauser and co-workers in an MD study of [bmim][CF$_3$COO].[80] The activation energies for reorientation dynamics from Arrhenius fits of the relaxation times were found to be 33.2 ± 1.1 and 9.9 ± 0.6 kJ mol^{-1} for the cations and the anions, respectively (Table 2). Again, the size and asymmetry of the cations explain their higher activation barrier; the nearly spherical anions can reorient in place without requiring a redistribution of free volume. The fast reorientation of the anions reduces the possibility of forming long-lasting hydrogen bonds, consistent with the short lifetime of hydrogen bonds discussed above.

D. Electrical Conductivity. The electrical (ionic) conductivity is an important transport property of ionic liquids from a practical point of view. Few of the existing models reproduce
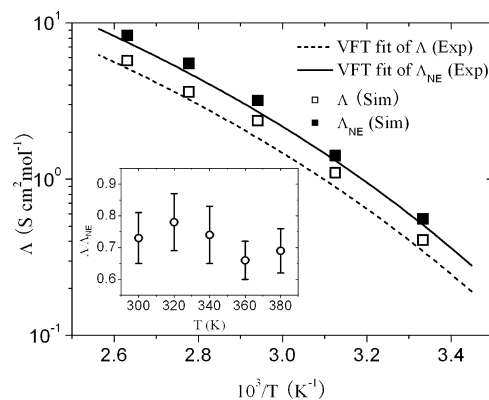

Figure 9. Molar ionic conductivity as function of temperature in comparison with experimental results which are presented as Vogel−Fulcher−Tamman (VFT) fits, $\Lambda = \Lambda_0 \exp(-B/(T - T_0))$ (see ref[20] for the fitting parameters). Inset: the ratio Λ/Λ_{NE} as function of temperature obtained in the present work. The Λ values were calculated according to eq 4 from the collective mean-square displacement curves by least-squares fitting lines to their linear regions: 1−5 ns (300 K), 0.5−2 ns (320 K), 0.5−2 ns (340 K), 0.5−1.5 ns (360 K), and 0.5−2.5 ns (380 K).

the conductivity satisfactorily,[81] which suggests a need for better molecular descriptions of ionic liquids. In this work, the molar conductivity has been computed for the present model from the collective mean-square displacement using the Einstein law:

$$\Lambda = \frac{N_0 e^2}{6nk_\mathrm{B}T}\lim_{t\to\infty}\frac{\mathrm{d}}{\mathrm{d}t}\sum_i\sum_j z_i z_j \langle [\mathbf{R}_i(t) - \mathbf{R}_i(0)]\cdot[\mathbf{R}_j(t) - \mathbf{R}_j(0)]\rangle \tag{4}$$

where N_0 is the Avogadro constant, k_B the Boltzmann constant, T the temperature, e the elementary charge, and n the number of ions. A charge z_i of ion i of ±1 was employed for the ions in this analysis of the conductivity, although the ion net charges of the force field used to calculate the electrostatic interactions were +0.8 and −0.8. The nitrogen atom carrying the butyl group was chosen as the reference atom for the cation position, while the phosphorus atom was chosen as the reference atom of the anion. $\mathbf{R}_i(t)$ refers to the position of ion i at time t, and the angle brackets denote an ensemble average.

We also calculated the molar conductivity in the Nernst−Einstein approximation Λ_{NE}, which essentially ignores the ion−ion coupling, both co-ion and counterion coupling, contained in the cross terms of the collective mean-square displacement $z_i z_j \langle [\mathbf{R}_i(t) - \mathbf{R}_i(0)]\cdot[\mathbf{R}_j(t) - \mathbf{R}_j(0)]\rangle$. This is given by

$$\Lambda_{NE} = \frac{N_0 e^2}{k_\mathrm{B}T}(D_{\text{anion}} + D_{\text{cation}}) \tag{5}$$

where D_{cation} and D_{anion} refer to the self or tracer diffusion coefficients of cations and anions, respectively.

The conductivities calculated from both the Einstein law (eq 4) and the Nernst−Einstein approximation (eq 5) are shown in Figure 9 in comparison with experimental measurements. For the investigated temperature range, conductivities calculated in this study are 12−29% higher than experimental values.[22] For instance, the molar conductivity at 300 K was found to be 0.56 S cm^2 mol^{-1} versus 0.51 S cm^2 mol^{-1} observed experimentally.[22] The molar conductivity values estimated by the Nernst−Einstein

(80) Schröder, C.; Rudas, T.; Neumayr, G.; Gansterer, W.; Steinhauser, O. *J. Chem. Phys.* **2007**, *127*, 044505.

(81) Monteiro, M. J.; Bazito, F. F. C.; Siqueira, L. J. A.; Ribeiro, M. C. C.; Torresi, R. M. *J. Phys. Chem. B* **2008**, *112*, 2102.

approximation are 7−18% higher than those estimated on the basis of NMR measurements of self-diffusion coefficients of cations and anions. Notwithstanding this difference, the present model signifies a large improvement compared to previous models for which the ionic conductivity was found to be 2 orders of magnitude lower than in experiment.[81] A quantity of interest is the ratio Λ/Λ_{NE} between the true conductivity Λ and the Nernst−Einstein estimate Λ_{NE}. The ionic conductivity Λ is a collective transport property which involves the correlated motion of all ions. The Nernst−Einstein approximation Λ_{NE}, on the other hand, assumes independent uncorrelated motion of the ions. Therefore, the ratio Λ/Λ_{NE} is a measure of the balance between correlated and uncorrelated motion of the ions.[82] A value $\Lambda/\Lambda_{NE} = 1$ would correspond to completely uncorrelated ion motion, while $\Lambda/\Lambda_{NE} = 0$ would indicate a highly collective motion where all the cations would follow the anions or vice versa.

The inset of Figure 9 shows the ratio Λ/Λ_{NE}. In our computations, the value of this ratio falls between 0.66 and 0.78 over the temperature range considered, which is in good agreement with the experimental value of about 0.67 (obtained from VFT fits of experimental data) for [bmim][PF₆] reported by Tokuda and co-workers.[22] It has been found empirically by Watanabe and co-workers[83] that, for a number of imidazolium-based ionic liquids, the Λ/Λ_{NE} ratio decreases with increasing basicity of the anion and with increasing alkyl chain length of the cation. For instance, [bmim][PF₆] exhibits a higher Λ/Λ_{NE} value than [bmim][CF₃SO₃], which has a Λ/Λ_{NE} value of 0.58,[83] as [PF₆] is a weaker base than [CF₃SO₃].

Up to now, we have successfully reproduced the ionic conductivity as well as the ratio Λ/Λ_{NE}. It has been suggested in some work that a Λ/Λ_{NE} value below 1 might indicate the existence of long-lived ion-pairs in ionic liquid systems.[21] However, no other experimental evidence has been found for the existence of ion-pairs in neat ionic liquid systems. The existence of ion-pairs is not evident in our MD results of previous sections either. Therefore, the molecular mechanism is worth examining, as it may be the cause for the ionic conductivity being lower than expected from the Nernst−Einstein approximation. This is the topic of the next section.

E. Ion-Pair Dissociation Dynamics. Analysis of the cation coordination number shows that the probabilities of finding a cation with four, five, six, and seven neighboring anions are 3%, 31%, 51%, and 15%, respectively, taking the first minimum of the center-of-mass RDF (Figure 4) at 0.76 nm as the coordination shell radius. The majority of cations are in contact with six anions.

The association/dissociation dynamics of cation−anion contacts was analyzed using a time correlation function similar to eqs 1 and 2:

$$S(t) = \frac{\langle \delta p(0) \delta P(t) \rangle}{\langle \delta p(0) \delta P(0) \rangle} = \frac{\langle p(0) P(t) \rangle - \langle p \rangle \langle P \rangle}{\langle p \rangle - \langle p \rangle \langle P \rangle} \approx \frac{\langle p(0) P(t) \rangle}{\langle p \rangle} \quad (6)$$

and

$$C(t) = \frac{\langle \delta p(0) \delta p(t) \rangle}{\langle \delta p^2 \rangle} = \frac{\langle p(0) p(t) \rangle - \langle p \rangle^2}{\langle p \rangle - \langle p \rangle^2} \approx \frac{\langle p(0) p(t) \rangle}{\langle p \rangle} \quad (7)$$

where the population variable $p(t)$ is unity when the ions are in contact at time t, according to the definition, and zero otherwise. For the survival index, $P(t) = 1$ holds if the tagged ion-pair
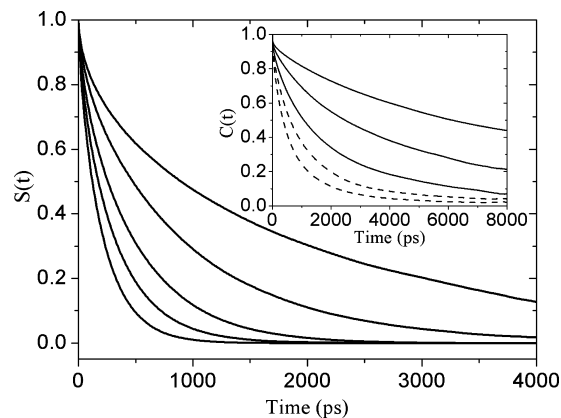

Figure 10. Time correlation functions of ion-pair dynamics $C(t)$ (inset, from top to bottom: 300, 320, 340, 360, and 380 K, respectively) and $S(t)$ for all investigated temperatures.

remains intact continuously until the time t, and $P(t) = 0$ otherwise. The angle brackets denote an average over all ion-pairs and all starting times. The average probability of an ion-pair is denoted as $\langle p \rangle$. According to the definition, $C(t)$ describes the probability that a particular tagged ion-pair is intact at time t, given that it was intact at time zero, while $S(t)$ provides a definition of the lifetime of a tagged ion-pair. The relaxation time of $C(t)$ is usually called the structural relaxation time (τ_R), and the relaxation time of $S(t)$ describes the average lifetime (τ_P) of ion-pairs.

Figure 10 shows the $C(t)$ and $S(t)$ at all temperatures investigated in this work. It can be seen that $S(t)$ decays faster than $C(t)$, as they are defined to describe different processes. Similar to the procedures followed in section B, we employ three weighted (with a total weight of one) exponentials to obtain the relaxation times of $S(t)$ and $C(t)$. By this approach, the lifetimes τ_P of ion-pairs were found to be 1.75, 0.82, 0.43, 0.29, and 0.20 ns at 300, 320, 340, 360, and 380 K, respectively, whereas the structural relaxation times (τ_R) were found to be 9.90, 4.82, 2.43, 1.52, and 0.96 ns. Good agreement with Arrhenius's law was found with activation energies of 25.9 ± 1.3 and 29.5 ± 1.5 kJ mol⁻¹ for $S(t)$ and $C(t)$, respectively (see Table 2 and Figure S2 in Supporting Information). The activation energy for $C(t)$ being higher than that for $S(t)$ results from the fact that $S(t)$ describes the first-time breaking of an ion-pair, while $C(t)$ describes a long-time structure relaxation which corresponds to the long-time diffusive motion, as also indicated by the relaxation time calculations. Compared to the binding energy of an isolated ion-pair in the gas phase, which ranges from 300 to 400 kJ/mol,[2,9,10,84] the activation energy of cation−anion contact found here is 1 order of magnitude lower. This is a consequence of the condensed environment rather than vacuum: if a cation loses one anion, its place will quickly be occupied by another one.

If the association into long-lived ion-pairs were responsible for the discrepancy between true conductivity and Nernst−Einstein conductivity, then these distinct pairs would have to travel jointly: they would migrate as a pair without breaking their contact. This can be studied by simulation. We analyze the translational mobility of two ions within their lifetimes: How

(82) Borodin, O.; Smith, G. D. *J. Phys. Chem. B* **2006**, *110*, 11481.
(83) Tokuda, H.; Tsuzuki, S.; Susan, A. B. H.; Hayamizu, K.; Watanabe, M. *J. Phys. Chem. B* **2006**, *110*, 19593.
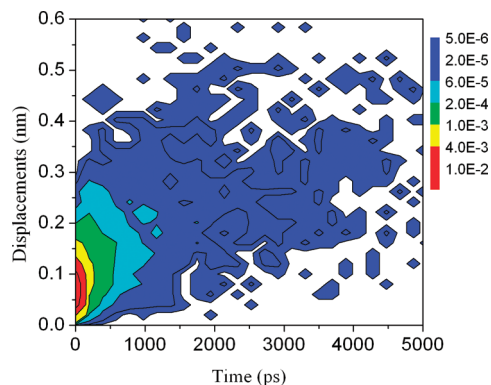(84) Tsuzuki, S.; Tokuda, H.; Hayamizu, K.; Watanabe, M. *J. Phys. Chem. B* **2005**, *109*, 16474.

Figure 11. Occurrence density of ion-pairs as functions of their lifetimes and displacements. The density is accumulated over 40 ns at 300 K. The plot unit (color code) is the number of occurrence of ion association per (0.004 nm × 8 ps).

far do they travel together before they break up? In the further analysis, a cation is said to form an ion-pair with an anion if their center-of-mass distance is less than or equal to 0.76 nm (the first coordination shell). This definition implies that every ion is always associated with several counterions. The position of each ion-pair was represented by the midpoint of the cation–anion center-of-mass distance. Figure 11 shows the distribution of the displacement of this position, which is reached at the time when the pair separates (i.e., its lifetime). The majority of ion-pairs have an extremely short lifetime of a few tens of picoseconds, during which they translate a distance of less than 0.2 nm. The distance traveled is therefore smaller than the ion–ion distance. Therefore, for most ion-pairs no lasting displacement is achieved before they separate. Larger displacements are obviously found for ion-pairs which have a longer lifetime. At 300 K, displacements of 0.4 nm with corresponding lifetimes of 3.5 ns are visible (see Figure 11), which change to 1.0 nm and 1.0 ns at 380 K (see Figure S3 in Supporting Information). However, the occurrence of long-lived ion-pairs is very low (note the logarithmic scale of the distribution). At higher temperature, the ion-pair displacements are larger in spite of their lifetime being lower. This is a consequence of the generally higher mobility. At 300 K, the longest lifetime found for any ion-pair was 24 ns, while the value at 380 K was much lower, 2.7 ns. The maximum displacements were 1.2 nm at 300 K and 2.3 nm at 380 K. It must be emphasized again that these extreme cases are statistically irrelevant. Therefore, the cation–anion contact is better described using the notion of *ion association* proposed by del Popolo et al.[18] instead of *ion-pair*.

On the basis of our analysis, we suggested that the reduction in conductivity (or deviation from the Nernst–Einstein approximation) results from the correlated motion of ions. Del Popolo and Voth suggested that subpicosecond dynamic coupling motion of neighboring ions might give rise to a reduction in conductivity.[27] However, as most ionic liquids are usually highly viscous at room temperature, all subpicosecond dynamics mostly relates to the local ballistic motion of neighboring ions. Our analysis reveals a temperature-dependent coupled motion of ions and their neighboring counterions over a time scale up to nanoseconds. A similar notion of the effects of coupled ionic motion on conductivity has long since been proposed for simple molten salts.[28,29,85] The presence of counterions serves as an

(85) Salanne, M.; Simon, C.; Turq, P.; Madden, P. A. *J. Phys. Chem. B* **2007**, *111*, 4678.

ionic atmosphere which causes a viscous drag on the central ion. This phenomenon, also known as the electrophoretic effect,[29] leads to a reduction in the mobility of ions and therefore in their contribution to conductivity.

Conclusions

In the present work, an ionic liquid system [bmim][PF$_6$] was studied by classical MD simulations based on an all-atom model. The purpose of this work was to characterize the cation–anion interactions through investigation of a number of structural and, more importantly, dynamic properties and their temperature dependence. The angle-dependent radial distribution functions describe the spatial preference of anions around cations. We did find hydrogen-bonding between cations (ring hydrogens) and anions (fluorines). However, the hydrogen bonds were found to be weaker than expected, as indicated by their short lifetimes. Hydrogen-bonding does not, therefore, govern the mutual dynamics of neighboring ions. The hydrogen bond lifetimes are less than 1 ps, whereas the lifetime of cation–anion contacts is in the range of nanoseconds. This is due to the fast (reorientation time below 10 ps) rotation of the PF$_6^-$ anion: It can rotate many times in place, thereby making and breaking hydrogen bonds to its symmetrically equivalent fluorine atoms, without moving translationally. We conclude that hydrogen-bonding exists in this ionic liquid but that it is far from dominating its structure and dynamics, as has sometimes been suggested.[12] The ionic liquid [bmim][PF$_6$] is certainly held together by Coulomb forces, not by hydrogen bonds. It is likely, but yet unproven, that this is the case for other ionic liquids, too.

Table 2. Activation Energies Related to Different Molecular Dynamics Processes, in Which Arrhenius Behavior Is Assumed[a]

process	E_A (kJ/mol)
cation reorientation	33.2 ± 1.1
anion reorientation	9.9 ± 0.6
H-bond lifetime	4.5–4.8
H-bond structural relaxation	9.8–16.1
ion-pair lifetime	25.9 ± 1.3
ion-pair structural relaxation	29.5 ± 1.5
cation diffusion	34.4 ± 1.5
anion diffusion	36.1 ± 1.9
mixed diffusion	35.1 ± 1.6
mixed diffusion (exp)	34.09 ± 0.02
conductivity	31.0 ± 2.2
conductivity (exp)	31.42 ± 0.02

[a] The experimental values for fitting are taken from ref 20.

The temperature dependence of different molecular processes is compared in Table 2. We report the activation energies E_A for the processes with Arrhenius behavior. For those processes, which deviate mildly from the Arrhenius law and show VFT behavior, we have nonetheless performed an Arrhenius fit to obtain an order of magnitude estimate of E_A for comparison. They separate the processes into three classes. The hydrogen-bond lifetimes form their own class with $E_A \approx 4.5$ kJ/mol. Hydrogen bonds are broken by librational motions without any lasting reorientation or displacement of the two partners. The second class consists of the anion reorientation and the structural correlation of hydrogen bonds. They have activation energies of about 10 kJ/mol. This supports the above explanation that anion in-place reorientation brings different fluorines into contact with a given ring hydrogen of the cation and thereby decorrelates the hydrogen bonds. The remaining processes, class three, involve a lasting translational displacement of ions. They have activation energies between 25 and 36 kJ/mol. Exchange of

counterions in an ion's solvation shell requires the same motion as the diffusion of ions or the conduction of charge. Cation reorientation falls into the same class, because the rotation of the long axis of the cation requires a molecular rearrangement of its solvation shell of an extent comparable to that necessary for the cation to perform a diffusive jump.

The transport parameters calculated with the present model (cation and anion tracer diffusion coefficients, conductivity) reproduce well the experimental data and their activation energies (Table 2). Moreover, it is observed that the true ionic conductivity is lower than the conductivity calculated from ion diffusion coefficients using the Nernst−Einstein approximation. This fact has also been found in experiments. We have carefully searched for the presence of long-lived ion-pairs, which would explain it, as a diffusing ion-pair contributes to the diffusion coefficient but not to net charge transport. However, we have not found a statistically relevant number of them. Equally, the vast majority of ions do not travel together as neutral ion-pairs, which has been suggested as an explanation of the failure of the Nernst−Einstein approximation.[21] It should also be noted that the observation of hydrogen bonds in infrared spectra[9,86] or in NMR[86] chemical shifts is not sufficient to support the existence of long-lived ion-pairs, as these two methods provide static averages over many ions and over the duration of the

experiment and do not yield information on hydrogen-bond dynamics. Our results do not confirm the previously[22] suggested role of subpicosecond dynamical correlation of the ions for the reduction of the conductivity, either. Instead, we suggest that long-time correlated motion of the ions, such as electrostatic drag,[29] is responsible for a conductivity which is lower than that from the Nernst−Einstein approximation.

Supporting Information Available: Absolute energies and optimized geometries of [bmim] cations and [PF₆] anions, as well as supporting figures. This information is available free of charge via the Internet at http://pubs.acs.org.

JA906337P

(86) Wulf, A.; Fumino, K.; Michalik, D.; Ludwig, R. *ChemPhysChem* **2007**, *8*, 2265.